Available online at www.sciencedirect.com

ScienceDirect

Mendeleev Commun., 2021, **31**, 836–838

Mendeleev Communications

Synthesis of germanium sols *via* thermal decomposition of gaseous germane

Alexander A. Vinokurov,* Konstantin O. Znamenkov and Sergey G. Dorofeev

Department of Chemistry, M. V. Lomonosov Moscow State University, 119991 Moscow, Russian Federation. Fax: +7 495 939 0998; e-mail: vinokuroff.aa@gmail.com

DOI: 10.1016/j.mencom.2021.11.022

A new approach to the synthesis of colloidal Ge nanoparticles in high-boiling solvent *via* thermal decomposition of germane is presented. Obtained products were analyzed by XRD, XRF, TEM, absorption spectrophotometry, Raman IR and PL spectroscopy. Ge nanoparticles have mean sizes about 4–5 nm, are apparently amorphous and nonspherical.

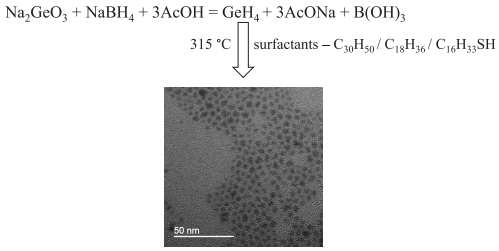

Keywords: germanium nanocrystals, germanium sols, germane, pyrolysis, amorphization, nanoparticles.

Germanium nanoparticles (NPs) are stable and nontoxic semiconductor material promising for photovoltaics[1,2] (*e.g.*, solar cells, LEDs, photodetectors), memory devices[3] and bioimaging[4] due to a narrow band gap (0.67 eV) and relatively large exciton Bohr radius (24 nm), which result in strong quantum confinement.[5] Ge nanoparticles NIR PL emissions can vary in the range of 800–1400 nm.[6]

Since 1991, when the the first luminescent germanium nanocrystals (NCs) immobilized in silica matrix were synthesized,[7] several approaches to creating Ge nanoparticles have been developed. Here we describe the reactions carried out in the solutions, which provide control of NCs size and their surface passivation. This allows us to vary the electronic properties of the material and gives way to further modifications of the formed nanoparticles. The common features of these approaches are the following: using nonpolar organic solvents [*e.g.* octadecene-1 (ODE), toluene]; temperatures up to 300 °C; an inert atmosphere (Ar, N_2) and strict control of oxygen- and water-free conditions.[8] There are five basic routes of the synthesis: (1) reduction of germanium halides (GeX_2 and GeX_4, X = Cl, Br, I) by hydrides or organometallic compounds;[9] (2) interaction of germanides M_xGe (M = Na, K, Mg) with ammonia salts[10] or germanium chloride $GeCl_4$;[11] (3) high pressure and temperature thermolysis of organogermanes (GeH_2Ph_2, $GeEt_4$);[12] (4) thermal decomposition of amidogermanes, *e.g.* $Ge[N(SiMe_3)_2]_2$;[13] (5) thermal reduction of coprecipitated GeO_2/SiO_2 sols with hydrogen, hydrides, amides, citrates, followed by HF etching to remove silicon dioxide from encapsulated Ge NCs.[14] However, these approaches are usually complex and require rare reagents. Hence, it would be useful to develop a new synthetic method to produce Ge NCs that does not utilize unstable precursors and requires more available reagents.

Here we report a new approach to creating Ge nanoparticles in organic high-boiling noncoordinating solvent (squalane) by thermal decomposition of gaseous germane (GeH_4) in the presence of surface stabilizers – surfactants.† Samples and experimental details are briefly presented in Table 1. High-boiling surfactants, squalene ($C_{30}H_{50}$) and ODE ($C_{18}H_{36}$), have been chosen, because alkenes can terminate H-passivated Ge NPs through hydrogermylation reaction.[15] It should be noted that preliminary experiments showed that synthesis in pure squalane, without addition of the surfactant, resulted in black precipitate of germanium powder, while synthesis in pure ODE or squalane–ODE solutions with high ODE concentrations (>10 mol%) did not reveal any precipitate or Ge sols. This can be due to 'consumption' of Ge seeds by the surfactant, preventing their growth. Aliphatic thiols, such as hexadecanethiol ($C_{16}H_{33}SH$), are widely used surfactants, they may stabilize Ge NCs that lose H-passivation.

As a result of pyrolysis of germane, yellow-brown colloidal solutions were obtained. Though sample 3, containing GeI_4, was dark brown. The intense coloration might be explained by higher

† Germanium nanoparticles were synthesized *via* thermal decomposition of gaseous germane GeH_4. GeH_4 was obtained through reduction of sodium germanate by $NaBH_4$ according to reaction $Na_2GeO_3 + NaBH_4 + 3AcOH = 3AcONa + GeH_4 + B(OH)_3$. The initial germanate was prepared by dissolving of GeO_2 (5 mmol) powder in 1 M NaOH (20 ml). Then $NaBH_4$ (30 mmol) was added to the alkaline germanate solution. The resulting mixture was further utilized in germane syntheses. The apparatus was washed by Ar, then Na_2GeO_3–$NaBH_4$ mixture (4 ml) was added dropwise to 100% AcOH (2 ml) within 5 min. The emitting GeH_4 was bubbled through reaction mixture along with Ar flow.

The reaction mixture was prepared by mixing of high-boiling squalane ($C_{30}H_{62}$) solvent (1.5 ml) with a surfactant (0.1 ml); decomposition temperature was 315 °C. Three surfactants were tested: squalene ($C_{30}H_{50}$), octadecene-1 ($C_{18}H_{36}$) and hexadecanethiol ($C_{16}H_{33}SH$). One of the experiments was perfomed in the presence of GeI_4, (0.01g) in order to check the assumption that germanium iodide would interact with germane by reaction $GeI_4 + GeH_4 = 2Ge + 4HI$, forming very small germanium seeds for better crystal growth.

Ge NCs were purified by consequent treatment with 'bad' solvent (8 : 1 acetone–THF mixture), centrifugation and redispersion in hexane.

Table 1 Experimental conditions, electronic band gap values and estimated particle diameters.

Sample	Surfactant	GeI_4	Growth time/min	E_g/eV	$d(E_g)$/nm
1	$C_{30}H_{50}$	-	10	1.39	5.5
2	$C_{18}H_{36}$	-	10	1.32	6.2
3	$C_{18}H_{36}$	+	10	1.34	6.0
4	$C_{16}H_{33}SH$	-	10	1.34	6.0
5	$C_{16}H_{33}SH$	-	0	1.32	6.1

content of nanoparticles in this solution, that were grown on numerous seeds formed at the reduction of GeI_4 by germane. Precipitation of nanoparticles caused many difficulties, and after centrifugation the product was generally an oily liquid instead of the precipitate.

After purification, resulting samples were characterized by XRD, XRF, TEM, as well as Raman, IR, absorption and PL spectra.‡ XRD patterns of Ge sols dried on Si(100) substrates showed diffuse amorphous halos corresponding to amorphous-like Ge nanoparticles. XRF revealed (see typical spectrum in Figure 1) that all samples contained only germanium (light elements, such as C, S, O and H, could not be detected under our experimental conditions). Raman spectra (Figure 2) for synthesized samples exhibited broad band at 270–290 cm^{-1}, characteristic of scattering from amorphous Ge phase.[16,17] In IR spectra for octadecene and thiol passivated samples (2 and 5, respectively) the following characteristic aliphatic vibrations were observed:[18] stretching ν(C–H) = 2960–2850 cm^{-1}, bending ν(C–H) = 1475, 1465, 1380 cm^{-1} and methylene rocking band at 720 cm^{-1}. There were no traces of Ge–H (2067 cm^{-1})[15] along with C=C–H (3100–3000 cm^{-1}) and S–H (2500 cm^{-1}) bands; thus, there were no significant quantities of unbonded surfactants in the samples. For sample 2, weak bands for Ge–O (910–870 cm^{-1}) and Ge–C (850 cm^{-1})[19] were detected, whereas for sample 5, only S–C at 633 cm^{-1} was identified. We can conclude that Ge nanoparticles are passivated by the introduced ligands, the NPs surface is not hydrogen-terminated and it is slightly oxidized, because the amount of germanium oxide is very low.

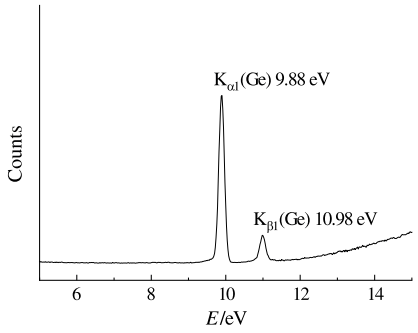

Figure 1 Typical XRF spectrum (sample 3).

‡ X-ray diffraction (XRD) patterns of Ge sols dried on Si(100) substrates were taken on a Rigaku D/MAX 2500 diffractometer using CuKα radiation (λ = 1.540598 Å). X-ray fluorescence (XRF) spectra were obtained on a Bruker M1 Mistral X-ray spectrometer. Raman spectra were recorded on i-Raman Plus spectrometer in backscattering geometry, 532 nm excitation laser (50 mW), excitation spot size 100 μm. Transmission electron microscopy (TEM) studies were performed using JEOL JEM 2100 microscope operating at 200 kV. IR spectra were taken on a Perkin-Elmer Frontier FTIR-spectrometer. Absorption spectra were measured at room temperature with a Varian Cary 50 spectrophotometer in a 1 cm quartz cuvette. Photoluminescence (PL) spectra were measured at room temperature with an Ocean Optics 4000 USB spectrometer calibrated using a 2600 K W-lamp. Excitation of PL was carried out using a 405 nm continuous laser LED (40 mW) and a 780 nm continuous laser LED (100 mW).

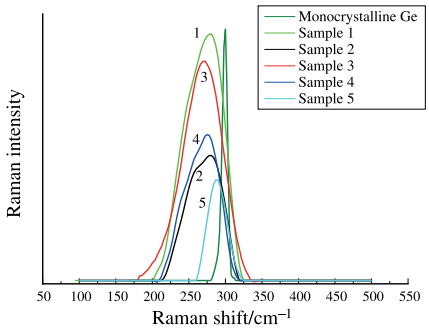

Figure 2 Raman spectra for monocrystalline Ge and synthesized samples.

Typical TEM images of samples 3, 4 and 5 are shown in Figure 3; particle size distribution is presented in Figure 4. The particles are either nonspherical or stuck together, especially in thiol-stabilized samples (4 and 5). Mean particles sizes are 4.3 ± 1.6, 5.3 ± 1.8 and 4.9 ± 1.6 nm for samples 3, 4 and 5, respectively. Obviously, the stabilizer or the reaction time do not affect the particle sizes.

Optical properties of the samples were studied by UV-NIR absorbance and PL spectroscopies. Absorption spectra [Figure 5(*a*)] of all three samples are very similar. Tauc plots of absorption data in Figure 5(*b*) allow us to determine band gap (E_g) of semiconductors. Linear extrapolation of absorption data in Tauc plot for indirect semiconductors gives us electronic band gap values inflated by phonon energy that, as it can be estimated from Raman spectrum for Ge NCs (Figure 2), is equal to ~0.033 eV. Adjusted E_g values and particles sizes $d(E_g)$ estimated by equation $E(d) = 1.05 + 10.3/d^2$ (according to Ö. Dag *et al.*[20]) are given in Table 1. Relatively large band gap values about 1.3–1.4 eV can be explained by quantum confinement effect along with the fact that nanoamorphous Ge has larger band gap (1.05 eV) than monocrystalline Ge (0.66 eV). It should be noted that particle sizes determined by direct TEM observations match well the values estimated by optical measurements. PL emission is barely noticeable for all samples.

Synthesized Ge nanoparticles are apparently amorphous. Amorphous Ge NPs were observed previously in other synthetic approaches using, for example, reduction of $GeCl_4$ by alkali metals at 270 °C[21] or ogranoalkali reagents,[22] thermal decomposition of various Ge^{II} precursors in ODE at 315 °C[23] or trichlorogermane in tri-*n*-octylamine.[24] In all instances experimental temperatures were not high. Therefore, the formation of amorphous phase may be related to the insufficient heating, as long as covalent nature of germanium requires high crystallization temperatures. Hence, carrying out reactions at

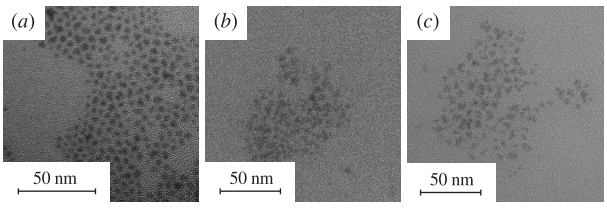

Figure 3 TEM images of samples: (*a*) 3, (*b*) 4, and (*c*) 5.

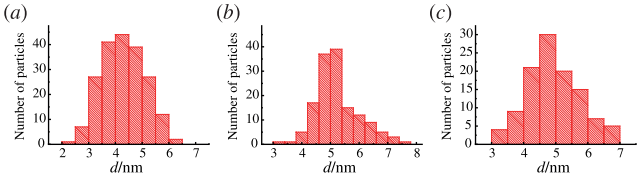

Figure 4 Particle size distribution for samples: (*a*) 3, (*b*) 4, and (*c*) 5.

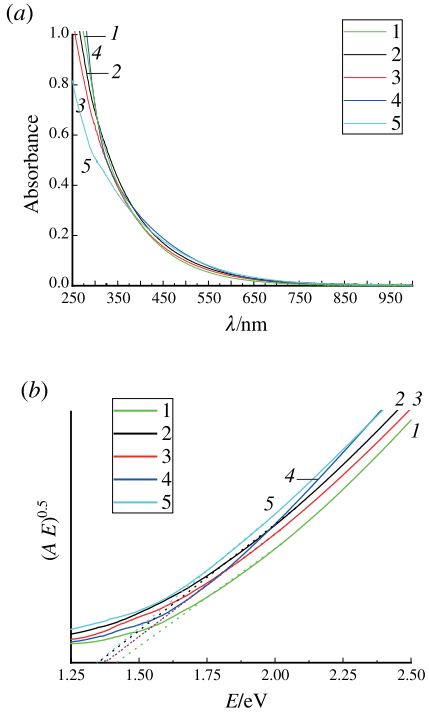

Figure 5 Optical properties of synthesized samples (*1*)–(*5*) 1–5, respectively: (*a*) absorption spectra, (*b*) linear extrapolation of absorption data in Tauc plot.

higher temperatures (up to 400 °C) in appropiate high-boiling solvents could be the target of further experiments. PL absence in our samples is explained by the presence of disordered amorphous phase, which provides a large number of point defects acting as electronic traps and quenching the luminescence. Optimization of synthetic protocol may be required to obtain crystallized samples possessing PL.

To conclude, we have developed a new approach to solution synthesis of germanium nanoparticles by thermal decomposition of gaseous germane in squalane solvent in the presence of high-boiling alkenes or thiol. Synthesized Ge nanoparticles have mean sizes about 4–5 nm, are apparently amorphous, nonspherical and possess low or almost zero PL, which is related to the large number of point defects in disordered amorphous phase. Further research would be needed to find-out the methods of better crystallization to improve the optical properties of Ge NCs.

References

1 B. Hekmatshoar, D. Shahrjerdi, M. Hopstaken, K. Fogel and D. K. Sadana, *Appl. Phys. Lett.*, 2012, **101**, 032102.
2 S. Siontas, D. Li, H. Wang, A. A. V. P. S., A. Zaslavsky and D. Pacifici, *Mater. Sci. Semicond. Process.*, 2019, **92**, 19.
3 D. V. Talapin, J. S. Lee, M. V. Kovalenko and E. V. Shevchenko, *Chem. Rev.*, 2010, **110**, 389.
4 J. Fan and P. K. Chu, *Small*, 2010, **6**, 2080.
5 A. L. Efros and M. Rosen, *Annu. Rev. Mater. Sci.*, 2000, **30**, 475.
6 W. Wang, B. Poudel, J. Y. Huang, D. Z. Wang, S. Kunwar and Z. F. Ren, *Nanotechnology*, 2005, **16**, 1126.
7 Y. Maeda, N. Tsukamoto, Y. Yazawa, Y. Kanemitsu and Y. Masumoto, *Appl. Phys. Lett.*, 1991, **59**, 3168.
8 B. F. P. McVey, S. Prabakar, J. J. Gooding and R. D. Tilley, *ChemPlusChem*, 2017, **82**, 60.
9 S. Prabakar, A. Shiohara, S. Hanada, K. Fujioka, K. Yamamoto and R. D. Tilley, *Chem. Mater.*, 2010, **22**, 482.
10 X. Ma, F. Wu and S. M. Kauzlarich, *J. Solid State Chem.*, 2008, **181**, 1628.
11 B. R. Taylor, S. M. Kauzlarich, H. W. H. Lee and G. R. Delgado, *Chem. Mater.*, 1998, **10**, 22.
12 X. Lu, B. A. Korgel and K. P. Johnson, *Nanotechnology*, 2005, **16**, S389.
13 H. Gerung, S. D. Bunge, T. J. Boyle, C. J. Brinker and S. M. Han, *Chem. Commun.*, 2005, 1914.
14 E. J. Henderson, M. Seino, D. P. Puzzo and G. A. Ozin, *ACS Nano*, 2010, **4**, 7683.
15 J. M. Buriak, *Chem. Rev.*, 2002, **102**, 1271.
16 M. Wihl, M. Cardona and J. Tauc, *J. Non-Cryst. Solids*, 1972, **8–10**, 172.
17 F. Evangelisti, M. Garozzo and G. Conte, *J. Appl. Phys.*, 1982, **53**, 7390.
18 B. H. Stuart, *Infrared Spectroscopy: Fundamentals and Applications*, John Wiley & Sons, Ltd., 2004.
19 E. Fok, M. Shih, A. Meldrum and J. G. C. Veinot, *Chem. Commun.*, 2004, 386.
20 Ö. Dag, E. J. Henderson and G. A. Ozin, *Small*, 2012, **8**, 921.
21 J. R. Heath, J. J. Shiang and A. P. Alivisatos, *J. Chem. Phys.*, 1994, **101**, 1607.
22 A. Kornowski, M. Giersig, R. Vogel, A. Chemseddine and H. Weller, *Adv. Mater.*, 1993, **5**, 634.
23 T. J. Boyle, L. J. Tribby, L. A. M. Ottley and S. M. Han, *Eur. J. Inorg. Chem.*, 2009, **36**, 5550.
24 N. Zaitseva, Z. R. Dai, C. D. Grant, J. Harper and C. Saw, *Chem. Mater.*, 2007, **19**, 5174.

Received: 10th March 2021; Com. 21/6486